

ADP-12-26/T793
 DESY 12-094
 Edinburgh 2012/07
 Liverpool LTH 946
 December 20, 2012

Isospin breaking in octet baryon mass splittings

R. Horsley^a, J. Najjar^b,
 Y. Nakamura^c, D. Pleiter^d, P. E. L. Rakow^e,
 G. Schierholz^f and J. M. Zanotti^g

– QCDSF-UKQCD Collaboration –

^a School of Physics and Astronomy, University of Edinburgh,
 Edinburgh EH9 3JZ, UK

^b Institut für Theoretische Physik, Universität Regensburg,
 93040 Regensburg, Germany

^c RIKEN Advanced Institute for Computational Science,
 Kobe, Hyogo 650-0047, Japan

^d Jülich Supercomputer Centre, Forschungszentrum Jülich,
 52425 Jülich, Germany

^e Theoretical Physics Division, Department of Mathematical Sciences,
 University of Liverpool, Liverpool L69 3BX, UK

^f Deutsches Elektronen-Synchrotron DESY,
 22603 Hamburg, Germany

^g CSSM, School of Chemistry and Physics, University of Adelaide,
 Adelaide SA 5005, Australia

Abstract

Using an $SU(3)$ flavour symmetry breaking expansion in the quark mass, we determine the QCD component of the nucleon, Sigma and Xi mass splittings of the baryon octet due to up-down (and strange) quark mass differences in terms of the kaon mass splitting. Provided the average quark mass is kept constant, the expansion coefficients in our procedure can be determined from computationally cheaper simulations with mass degenerate sea quarks and partially quenched valence quarks. Both the linear and quadratic terms in the $SU(3)$ flavour symmetry breaking expansion are considered; it is found that the quadratic terms only change the result by a few percent, indicating that the expansion is highly convergent.

1 Introduction

The masses of the baryon octet are now very accurately known, with results given in the Particle Data Group [1] as

$$\begin{aligned} M_n^{\text{exp}} &= 0.939565346(23) \text{ GeV}, & M_p^{\text{exp}} &= 0.938272013(23) \text{ GeV}, \\ M_{\Sigma^-}^{\text{exp}} &= 1.197449(30) \text{ GeV}, & M_{\Sigma^+}^{\text{exp}} &= 1.18937(7) \text{ GeV}, \\ M_{\Xi^-}^{\text{exp}} &= 1.32171(7) \text{ GeV}, & M_{\Xi^0}^{\text{exp}} &= 1.31486(20) \text{ GeV}, \end{aligned} \quad (1)$$

around the outer ring of the octet and

$$M_{\Sigma^0}^{\text{exp}} = 1.192642(24) \text{ GeV}, \quad M_{\Lambda}^{\text{exp}} = 1.115683(6) \text{ GeV}, \quad (2)$$

at the centre. Isospin breaking effects (i.e. $u - d$ quark mass differences and electromagnetic effects) are responsible for the nucleon, $n - p$, Sigma, $\Sigma^- - \Sigma^+$, and Xi, $\Xi^- - \Xi^0$, mass splittings

$$\begin{aligned} (M_n - M_p)^{\text{exp}} &= 1.293333(33) \text{ MeV}, \\ (M_{\Sigma^-} - M_{\Sigma^+})^{\text{exp}} &= 8.079(76) \text{ MeV}, \\ (M_{\Xi^-} - M_{\Xi^0})^{\text{exp}} &= 6.85(21) \text{ MeV}. \end{aligned} \quad (3)$$

These are very small differences (particularly for the $n - p$ mass splitting), ranging from about 0.15% to 0.7% of the baryon mass. (We shall not be considering the $\Sigma^0 - \Lambda$ mass splitting here as these particles have the same quantum numbers and mix if isospin is violated.) In this article we shall be only looking at the hadronic or QCD contribution to these mass splittings, i.e. we are not going to consider electromagnetic effects. Both effects are small perturbations and can simply be added together. In the case of the $n - p$ splitting we can argue that the hadronic effect is larger because the electromagnetic effect would tend to make the proton heavier than the neutron (as u quarks repel more than d quarks) which is not the case in the real world. There have been several previous lattice determinations of the QCD contribution to these mass splittings, e.g. [2, 3, 4], and also several lattice computations of the electromagnetic contribution, e.g. [3, 5, 6, 7, 8, 9, 10]. Non-lattice determinations include [11].

In Fig. 1 we sketch the lowest octet for the spin $\frac{1}{2}$ baryons plotted in the $I_3 - Y$ plane. The particles on the outer ring, namely the $n(ddd)$, $p(uud)$, $\Sigma^+(dds)$, $\Sigma^-(uus)$ and $\Xi^-(ssd)$, $\Xi^0(ssu)$ all consist of combinations of aab quarks (where we shall use the notation of denoting a quark, q , by a, b, \dots which can be the up u , down d or strange s quark). In this notation a are the flavour doubly represented quarks, while b is the flavour singly represented quark. At the centre of the octet we have two states, $\Lambda(uds)$ and $\Sigma^0(uds)$, with the same quark content – u, d and s , but different wavefunctions.

In [12, 13] we described a method for extrapolating from the $SU(3)$ flavour symmetric point (where we have three mass-degenerate quarks) to the physical

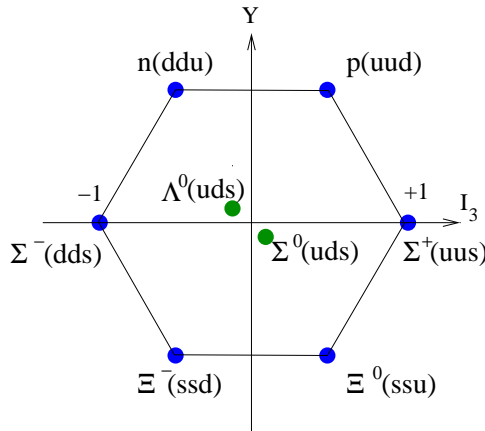


Figure 1: The lowest octet for the spin $\frac{1}{2}$ baryons plotted in the I_3 - Y plane.

point, keeping the average of the quark masses constant. The form of the $SU(3)$ flavour symmetry breaking expansion was developed both for non-degenerate u, d quark masses and for degenerate u, d quark masses. In [13] numerical simulations were performed for $2 + 1$ flavours, i.e. with two degenerate light quark masses. Thus, effectively the mass ‘average’ of the n, p baryon, and the Σ^+, Σ^- and Ξ^-, Ξ^0 baryons were considered. However, as the coefficients of the quark mass flavour symmetry are just functions of the average quark mass, the expansion coefficients do not change from using non-degenerate to 2 or 3 mass degenerate quarks provided that the average quark mass is kept constant [13]. This gives us the opportunity to investigate isospin splittings, i.e. when the u quark mass is different to the d quark mass, using only results from $2+1$ or 3 flavour simulations.

As the baryon mass differences (e.g. $n - p$) depend on the $u - d$ mass difference and are thus small, we find that it is sufficient to consider the $SU(3)$ flavour symmetry breaking expansion in the quark mass including both linear terms (leading order, LO) and quadratic terms (next to leading order, NLO). These LO and NLO terms were given in [13].

We saw little curvature in hadron masses in the quark mass range considered in [13] (see also section 6), namely, from the three degenerate flavour pion mass at ~ 411 MeV to the physical pion mass ~ 140 MeV, so we conclude that a much larger quark mass range is needed to reliably determine curvature. We achieve this larger range by extending the numerical results to ‘*partially quenched*’ or PQ quark masses (where the valence quark masses do not have to be the same as the sea or dynamical quark masses) with a spread of quark masses from about one third of the strange quark mass up to the charmed quark mass. We also consider part of the next to next to leading order (NNLO) (cubic terms) in the $SU(3)$ flavour symmetry expansion. (The NNLO terms were also indicated in [13]; we have now completed this computation, [14].) Thus we can consider a large quark

mass range to be able to determine the NLO or quadratic terms more accurately, using the NNLO terms as a ‘control’.

Chiral perturbation theory looks at the breaking of the chiral $SU(3)$ group by the quark masses - its expansion parameter is the quark mass itself, or equivalently, the masses of the pseudoscalar mesons. We are following an older strand, going back to Gell-Mann and Okubo [15, 16] of looking at the breaking of the non-chiral $SU(3)$ symmetry, by quark mass differences. In chiral perturbation theory the expansion is about the point where all three quarks are massless; here we expand about a point where the three quarks have equal (non-zero) masses each about a third of the physical strange quark mass.

As well as the baryon $SU(3)$ octet flavour expansion, we will also need the values of the quark mass corresponding to the physical point. We can achieve this by considering the equivalent $SU(3)$ flavour expansion, but now for the pseudoscalar meson octet. The same procedure as for the baryon octet is required: first the $SU(3)$ flavour expansion coefficients must be determined and then the experimental values of the masses of the K^0 , K^+ and π^+ mesons can be used to determine the required physical quark mass point. These can then be used, together with the $SU(3)$ baryon octet flavour expansion, to determine the mass splittings for the baryon octet.

We shall find that the LO term is dominant (both for the baryon and pseudoscalar octets) and so the NLO (and NNLO corrections) may be taken as an indication that our $SU(3)$ flavour symmetry breaking expansion appears to be a highly convergent series. (This point is further discussed in Appendix A.)

2 Octet Baryons

Before discussing partial quenching, we first consider the case where the valence quark masses are the same as the sea quark masses, the so-called ‘*unitary line*’. The $SU(3)$ flavour symmetry breaking expansion, [13], for all of the outer ring octet baryons consisting of a pair of identical flavour quarks and a third, different quark can be compactly written up to NLO as

$$\begin{aligned}
 M^2(aab) &= M_0^2 + A_1(2\delta m_a + \delta m_b) + A_2(\delta m_b - \delta m_a) \\
 &\quad + B_0\frac{1}{6}(\delta m_a^2 + \delta m_d^2 + \delta m_s^2) \\
 &\quad + B_1(2\delta m_a^2 + \delta m_b^2) + B_2(\delta m_b^2 - \delta m_a^2) + B_3(\delta m_b - \delta m_a)^2,
 \end{aligned}
 \tag{4}$$

with quarks $q = a, b, \dots$ from (u, d, s) , where

$$\delta m_q = m_q - \bar{m}, \quad \bar{m} = \frac{1}{3}(m_u + m_d + m_s).
 \tag{5}$$

We shall consider the $SU(3)$ flavour symmetry breaking expansion of $M^2(aab)$ [17], rather than $M(aab)$. Of course from the viewpoint of the $SU(3)$ flavour symmetry breaking expansion any function $f(M)$ could be considered. For fitting

over a small quark mass range, a linear function is sufficient; for the large quark mass range considered in section 3.2 a better fit to the numerical data was found using $M^2(aab)$ rather than $M(aab)$.

Note that $M_0^2, A_1, A_2, B_0, \dots, B_3$ all depend on the average quark mass \overline{m} , which will be held constant in the following simulations. Keeping \overline{m} constant reduces the number of coefficients that must be determined (and indeed makes the computation tractable).

From Fig. 1 we see that as there are six different masses on the baryon outer ring but just two linear parameters in LO, the fits are highly constrained. At the next order, NLO, in eq. (4) we are allowed four coefficients for the quadratic terms.

We have in addition the trivial constraint

$$\delta m_u + \delta m_d + \delta m_s = 0, \quad (6)$$

so we can eliminate one of these quantities if we wish to.

Thus, to determine the octet baryon masses, we first have to determine the expansion coefficients and second we need to know the physical quark masses. In the following we shall denote the physical point by a star *. We thus have two distinct computations. As we shall see, the determination of the coefficients is helped by PQ simulations, while δm_q^* can be found by considering equivalent expansions for the pseudoscalar meson octet.

A further problem is that the scale must be determined. As discussed in [13], flavour blind (or gluonic) quantities are suitable. We denote these generically by X . One useful type of flavour blind quantity can be considered as the ‘centre of mass’ of the multiplet. Thus for the baryon octet, one possibility is¹

$$X_N^2 = \frac{1}{6}(M_p^2 + M_n^2 + M_{\Sigma^+}^2 + M_{\Sigma^-}^2 + M_{\Xi^0}^2 + M_{\Xi^-}^2). \quad (7)$$

At the physical point, from eq. (1), this gives

$$X_N^{\text{exp}} = 1.1610 \text{ GeV}. \quad (8)$$

In general for the $SU(3)$ flavour breaking symmetry expansion we have from eq. (4),

$$\begin{aligned} X_N^2 &= M_0^2 + (\frac{1}{6}B_0 + B_1 + B_3)(\delta m_u^2 + \delta m_d^2 + \delta m_s^2) \\ &= M_0^2 + O(\delta m_q^2). \end{aligned} \quad (9)$$

Upon adding the masses the A_2 and B_2 terms vanish; while the A_1 term vanishes upon using the constraint equation, eq (6), and thus this leads to the vanishing of the linear term in the quark mass. (This is indeed true for all flavour blind quantities.)

¹Another independent possibility would be $X_\Lambda^2 = \frac{1}{2}(M_\Lambda^2 + M_{\Sigma^0}^2)$.

Scale independent quantities can now be constructed by considering the ratio $M^2(ab)/X_N^2$. Expanding to NLO order in the quark mass, eq. (4) retains the same pattern and becomes

$$\begin{aligned}\tilde{M}^2(ab) &= 1 + \tilde{A}_1(2\delta m_a + \delta m_b) + \tilde{A}_2(\delta m_b - \delta m_a) \\ &\quad - (\tilde{B}_1 + \tilde{B}_3)(\delta m_u^2 + \delta m_d^2 + \delta m_s^2) \\ &\quad + \tilde{B}_1(2\delta m_a^2 + \delta m_b^2) + \tilde{B}_2(\delta m_b^2 - \delta m_a^2) + \tilde{B}_3(\delta m_b - \delta m_a)^2,\end{aligned}\tag{10}$$

where a $\tilde{}$ on a hadron mass means that it has been divided by X_N , so $\tilde{M} = M/X_N$ while a $\tilde{}$ on the expansion coefficients means that they have been divided by M_0^2 , for example $\tilde{A}_1 \equiv A_1/M_0^2$. From eq. (9) we see that we have effectively replaced the $\frac{1}{6}\tilde{B}_0$ term by $-(\tilde{B}_1 + \tilde{B}_3)$. (However, this will not be important in the case discussed here; as for mass differences, these terms cancel again.)

Alternatively we can re-write eq. (10) as

$$\begin{aligned}\tilde{M}(ab) &= 1 + \tilde{A}'_1(2\delta m_a + \delta m_b) + \tilde{A}'_2(\delta m_b - \delta m_a) \\ &\quad - \frac{1}{2}(\tilde{B}_1 + \tilde{B}_3)(\delta m_u^2 + \delta m_d^2 + \delta m_s^2) \\ &\quad + \tilde{B}'_1(2\delta m_a^2 + \delta m_b^2) + \tilde{B}'_2(\delta m_b^2 - \delta m_a^2) + \tilde{B}'_3(\delta m_b - \delta m_a)^2,\end{aligned}\tag{11}$$

(essentially the equivalent $SU(3)$ flavour symmetry breaking expansion for M rather than M^2) with

$$\begin{aligned}\tilde{A}'_1 &= \frac{1}{2}\tilde{A}_1, \\ \tilde{A}'_2 &= \frac{1}{2}\tilde{A}_2, \\ \tilde{B}'_1 &= \frac{1}{2}(\tilde{B}_1 - \frac{3}{4}\tilde{A}_1^2), \\ \tilde{B}'_2 &= \frac{1}{2}(\tilde{B}_2 - \frac{3}{4}\tilde{A}_1\tilde{A}_2), \\ \tilde{B}'_3 &= \frac{1}{2}(\tilde{B}_3 + \frac{1}{4}(2\tilde{A}_1 - \tilde{A}_2)(\tilde{A}_1 + \tilde{A}_2)).\end{aligned}\tag{12}$$

Although eq. (11) looks complicated, we shall only be interested in mass differences, which simplify the expressions. Writing the flavour expansions as a Taylor series in $\delta m_d \pm \delta m_u$ we find to NLO

$$\begin{aligned}\tilde{M}_n - \tilde{M}_p &= \tilde{M}(ddu) - \tilde{M}(uud) \\ &= (\delta m_d - \delta m_u) \left[\tilde{A}'_1 - 2\tilde{A}'_2 + (\tilde{B}'_1 - 2\tilde{B}'_2)(\delta m_d + \delta m_u) \right],\end{aligned}\tag{13}$$

together with

$$\begin{aligned}\tilde{M}_{\Sigma^-} - \tilde{M}_{\Sigma^+} &= \tilde{M}(dds) - \tilde{M}(uus) \\ &= (\delta m_d - \delta m_u) \left[2\tilde{A}'_1 - \tilde{A}'_2 + (2\tilde{B}'_1 - \tilde{B}'_2 + 3\tilde{B}'_3)(\delta m_d + \delta m_u) \right],\end{aligned}\tag{14}$$

and

$$\begin{aligned}\tilde{M}_{\Xi^-} - \tilde{M}_{\Xi^0} &= \tilde{M}(ssd) - \tilde{M}(ssu) \\ &= (\delta m_d - \delta m_u) \left[\tilde{A}'_1 + \tilde{A}'_2 + (\tilde{B}'_1 + \tilde{B}'_2 + 3\tilde{B}'_3)(\delta m_d + \delta m_u) \right],\end{aligned}\tag{15}$$

where the constraint in eq. (6) has been used to eliminate δm_s . These equations represent the different types of isospin differences possible for the baryon octet and are valid over a range of quark masses. We shall consider them from the flavour symmetric point down to the physical point, determined by $\delta m_d^* - \delta m_u^*$ and $\delta m_d^* + \delta m_u^* = -\delta m_s^*$, δm_q^* being the physical point (which has to be determined).

We have a check of these formulas, since the Coleman-Glashow relation [18] should hold at this order,

$$(\tilde{M}_n - \tilde{M}_p) - (\tilde{M}_{\Sigma^-} - \tilde{M}_{\Sigma^+}) + (\tilde{M}_{\Xi^-} - \tilde{M}_{\Xi^0}) = O(\delta m_q^3), \quad (16)$$

which is indeed satisfied by eqs. (13)–(15).

We can find relations between isospin violation caused by $m_d - m_u$ and to the $SU(3)$ violation caused by $m_s - m_u$, $m_s - m_d$ if we make any S_3 transformation that changes the strange quark into a light quark and vice versa (for example $u \rightarrow s \rightarrow d$ or $d \leftrightarrow s$); see Fig. 2. (S_3 is the symmetry group of the equilateral

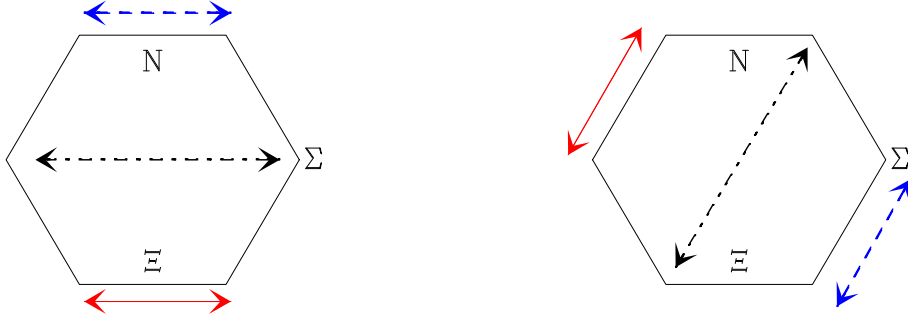


Figure 2: Permutation group transformations link the isospin violation caused by $m_d - m_u$ to the $SU(3)$ violation caused by $m_s - m_u$, $m_s - m_d$. The neutron-proton mass difference, $M_n - M_p$, dashed line, is mapped to $M_{\Xi^0} - M_{\Sigma^+}$; the Σ splitting, $M_{\Sigma^-} - M_{\Sigma^+}$, maps to $M_{\Xi^-} - M_p$ dot-dashed line; and $M_{\Xi^-} - M_{\Xi^0}$ is related to $M_{\Sigma^-} - M_n$, full line.

triangle and a subgroup of $SU(3)$.) Applying the transformation $d \leftrightarrow s$ on both sides of eqs. (13)–(15) we find to NLO

$$\begin{aligned} \tilde{M}_{\Xi^0} - \tilde{M}_{\Sigma^+} &= (\delta m_s - \delta m_u) \left[\tilde{A}'_1 - 2\tilde{A}'_2 + (\tilde{B}'_1 - 2\tilde{B}'_2)(\delta m_s + \delta m_u) \right], \quad (17) \\ \tilde{M}_{\Xi^-} - \tilde{M}_p &= (\delta m_s - \delta m_u) \left[2\tilde{A}'_1 - \tilde{A}'_2 + (2\tilde{B}'_1 - \tilde{B}'_2 + 3\tilde{B}'_3)(\delta m_s + \delta m_u) \right], \\ \tilde{M}_{\Sigma^-} - \tilde{M}_n &= (\delta m_s - \delta m_u) \left[\tilde{A}'_1 + \tilde{A}'_2 + (\tilde{B}'_1 + \tilde{B}'_2 + 3\tilde{B}'_3)(\delta m_s + \delta m_u) \right]. \end{aligned}$$

3 Determining the expansion coefficients

We now first find the \tilde{A}_1 , \tilde{A}_2 and $\tilde{B}_1, \dots, \tilde{B}_3$ coefficients.

3.1 Partially quenched octet baryons

Let us now generalise the previous results to the case when the valence quarks do not have to have the same mass as the sea quarks (i.e. we leave the unitary line). We have also generalised eq. (65) of [13] from NLO to NNLO [14]. We find

$$\begin{aligned}
M^2(aab) = & M_0^2 + A_1(2\delta\mu_a + \delta\mu_b) + A_2(\delta\mu_b - \delta\mu_a) \\
& + \frac{1}{6}B_0(\delta m_u^2 + \delta m_d^2 + \delta m_s^2) \\
& + B_1(2\delta\mu_a^2 + \delta\mu_b^2) + B_2(\delta\mu_b^2 - \delta\mu_a^2) + B_3(\delta\mu_b - \delta\mu_a)^2 \\
& + C_0\delta m_u\delta m_d\delta m_s \\
& + [C_1(2\delta\mu_a + \delta\mu_b) + C_2(\delta\mu_b - \delta\mu_a)](\delta m_u^2 + \delta m_d^2 + \delta m_s^2) \\
& + C_3(\delta\mu_a + \delta\mu_b)^3 + C_4(\delta\mu_a + \delta\mu_b)^2(\delta\mu_a - \delta\mu_b) \\
& + C_5(\delta\mu_a + \delta\mu_b)(\delta\mu_a - \delta\mu_b)^2 + C_6(\delta\mu_a - \delta\mu_b)^3, \tag{18}
\end{aligned}$$

where a, b, \dots now denote three valence quarks of arbitrary mass, and we have defined

$$\delta\mu_q = \mu_q - \bar{m} \quad q \in \{a, b, \dots\}, \tag{19}$$

where μ_q is the valence quark mass. In distinction to the sea quarks, there is no restriction of the form of eq. (6) on the values of valence quark masses. The numerical values of the $M_0^2, A_1, A_2, B_0, B_1, \dots, B_3$ and C_0, \dots, C_6 coefficients are the same for PQ as for the unitary case.

While we see that this is a relatively straightforward generalisation of eq. (4), we note that the term proportional to B_0 remains unchanged. In addition the C_0 term also depends entirely on sea terms, while the C_1 and C_2 terms are a mixture of sea and valence terms. Thus if we wish to determine these coefficients we must vary the sea quark masses; to determine the other coefficients it is sufficient to vary the valence quark masses alone, while keeping the sea quark masses constant. So this gives the possibility of extending the (computationally expensive) sea quark mass simulations with (computationally cheaper) valence quark mass simulations to determine most of the coefficients. If we work on a single sea background, then the C_0 term can be absorbed into the M_0^2 term, while the C_1 and C_2 terms can be absorbed into the A_1 and A_2 terms. If we vary the sea quark masses this allows a determination of these coefficients. However due to the constraint $\bar{m} = \text{const.}$, or equivalently eq. (6), δm_q cannot vary much and we know from [13] that in this range the LO dominates, so these coefficients are difficult to determine and contribute just noise. So practically we shall ignore these terms in fits. (Alternatively, the constraint $\bar{m} = \text{const.}$ could be relaxed, but then we have additional expansion coefficients, which we wish to avoid.) Thus in this article we regard the NNLO terms as ‘control’ on the LO and NLO terms.

As discussed in section 2, we can consider scale independent quantities. Thus in analogy to eq. (11) we have

$$\tilde{M}^2(aab) = 1 + \tilde{A}_1(2\delta\mu_a + \delta\mu_b) + \tilde{A}_2(\delta\mu_b - \delta\mu_a)$$

$$\begin{aligned}
& - (\tilde{B}_1 + \tilde{B}_3)(\delta m_u^2 + \delta m_d^2 + \delta m_s^2) \\
& + \tilde{B}_1(2\delta\mu_a^2 + \delta\mu_b^2) + \tilde{B}_2(\delta\mu_b^2 - \delta\mu_a^2) + \tilde{B}_3(\delta\mu_b - \delta\mu_a)^2 \\
& + (\tilde{C}_3 - 3\tilde{C}_5)\delta m_u \delta m_d \delta m_s \\
& + \left[\tilde{C}_1(2\delta\mu_a + \delta\mu_b) + \tilde{C}_2(\delta\mu_b - \delta\mu_a) \right] (\delta m_u^2 + \delta m_d^2 + \delta m_s^2) \\
& + \tilde{C}_3(\delta\mu_a + \delta\mu_b)^3 + \tilde{C}_4(\delta\mu_a + \delta\mu_b)^2(\delta\mu_a - \delta\mu_b) \\
& + \tilde{C}_5(\delta\mu_a + \delta\mu_b)(\delta\mu_a - \delta\mu_b)^2 + \tilde{C}_6(\delta\mu_a - \delta\mu_b)^3, \tag{20}
\end{aligned}$$

(where X_N always depends just on the sea quarks and is given by the NNLO extension of eq. (9)).

Furthermore, these equations remain valid if two of the sea quarks are degenerate in mass, i.e. $m_u = m_d \equiv m_l$, the crucial point being that \overline{m} must remain constant (as all the coefficients are functions of \overline{m}). This means that from dynamical 2 + 1 flavour simulations we can determine the u - d mass splittings. The only change to eq. (20) when $m_u = m_d$ is that some terms become slightly simpler,

$$\delta m_u^2 + \delta m_d^2 + \delta m_s^2 \rightarrow 6\delta m_l^2, \quad \delta m_u \delta m_d \delta m_s \rightarrow -2\delta m_l^3, \tag{21}$$

where we have used the constraint equation, (6), which now becomes

$$\delta m_s = -2\delta m_l. \tag{22}$$

This gives

$$\begin{aligned}
\tilde{M}^2(aab) &= 1 + \tilde{A}_1(2\delta\mu_a + \delta\mu_b) + \tilde{A}_2(\delta\mu_b - \delta\mu_a) \\
& - 6(\tilde{B}_1 + \tilde{B}_3)\delta m_l^2 \\
& + \tilde{B}_1(2\delta\mu_a^2 + \delta\mu_b^2) + \tilde{B}_2(\delta\mu_b^2 - \delta\mu_a^2) + \tilde{B}_3(\delta\mu_b - \delta\mu_a)^2 \\
& - 2(\tilde{C}_3 - 3\tilde{C}_5)\delta m_l^3 \\
& + 6 \left[\tilde{C}_1(2\delta\mu_a + \delta\mu_b) + \tilde{C}_2(\delta\mu_b - \delta\mu_a) \right] \delta m_l^2 \\
& + \tilde{C}_3(\delta\mu_a + \delta\mu_b)^3 + \tilde{C}_4(\delta\mu_a + \delta\mu_b)^2(\delta\mu_a - \delta\mu_b) \\
& + \tilde{C}_5(\delta\mu_a + \delta\mu_b)(\delta\mu_a - \delta\mu_b)^2 + \tilde{C}_6(\delta\mu_a - \delta\mu_b)^3, \tag{23}
\end{aligned}$$

with

$$X_N^2 = \frac{1}{3}(M^2(lll) + M^2(lls) + M^2(ssl)). \tag{24}$$

(For a quark mass-degenerate 3 flavour simulation eq. (23) simplifies further as $\delta m_l = 0 = \delta m_s$.) In other words, using eq. (23) gives us all the information we need to find the quark mass contribution relevant for the 1 + 1 + 1 case.

3.2 Numerical results

Simulations have been performed using $N_f = 2+1$ $O(a)$ improved clover fermions [19] at $\beta = 5.50$ and on $32^3 \times 64$ lattice sizes, as described in more detail in

[13]. Errors given here are statistical (using $\sim O(1500)$ configurations); possible systematic errors are discussed in Appendix A and incorporated into the final results in section 7.

A particular starting value for the degenerate sea quark mass, m_0 , is chosen on the $SU(3)$ flavour symmetric line, and the subsequent sea quark mass points m_l , m_s have then been arranged in the various simulations to have constant \overline{m} ($= m_0$). This ensures that the expansion coefficients do not change. It was found in [13] that a linear fit provides a good description of the numerical data over the relatively short distance from the symmetric point down to the physical pion mass. This helped us in choosing the initial point on the $SU(3)$ flavour symmetric line to give a path that hits (or is very close to) the physical point.

In a little more detail, the bare quark masses in lattice units are defined as

$$m_q = \frac{1}{2} \left(\frac{1}{\kappa_q} - \frac{1}{\kappa_{0;c}} \right) \quad \text{with } q \in \{l, s, 0\}, \quad (25)$$

(together with eq. (5) for δm_q) with the index $q = 0$ denoting the common mass degenerate quarks along the $SU(3)$ flavour symmetric line, and where vanishing of the quark mass along this line determines $\kappa_{0;c}$. Keeping $\overline{m} = \text{constant} \equiv m_0$ gives

$$\kappa_s = \frac{1}{\frac{3}{\kappa_0} - \frac{2}{\kappa_l}}. \quad (26)$$

So once we decide on a κ_l this then determines κ_s . Note that $\kappa_{0;c}$ drops out of eq. (26), so we do not need its explicit value. The initial $SU(3)$ flavour symmetric κ_0 value chosen here, namely $\kappa_0 = 0.12090$, [13] is very close to a point on the path that leads to the physical point. The constancy of flavour singlet quantities over the range from the $SU(3)$ flavour symmetric line down to the physical point [13], leads directly from X_π to an estimate for the pion mass of ~ 411 MeV (i.e. eq. (47)) and similarly from X_N a value of the lattice spacing of $a \sim 0.079$ fm.

While, as discussed earlier, simulations between the $SU(3)$ flavour symmetric point and the physical point are in principle enough to determine the linear and quadratic expansion coefficients, in practice the range is not sufficiently large to reliably determine the quadratic terms. In order to determine the quadratic coefficients more precisely, additional PQ simulations have been performed on the set of gauge configurations that have all three sea quark masses equal, i.e. at the $SU(3)$ flavour symmetric point $\kappa_0 = 0.12090$. For these particular simulations $\delta m_l = 0 = \delta m_s$ automatically. μ_q is defined identically to m_q , eq (25), by replacing $m_q \rightarrow \mu_q$ with $q \in \{a, b, \dots\}$ together with eq. (19) for $\delta \mu_q$ so that

$$\delta \mu_q = \mu_q - \overline{m}, \quad \mu_q = \frac{1}{2} \left(\frac{1}{\kappa_q} - \frac{1}{\kappa_{0;c}} \right). \quad (27)$$

We have chosen a wide range of PQ masses starting from a slightly heavier mass than m_0 (to avoid any possibility of so-called ‘exceptional configurations’) and

reaching up to masses $\sim m_{charm}$. The values are given in Appendix B in Table 4. A direct fit is made to these PQ masses, the unitary masses of [13], which all have the same fixed \overline{m} , and additionally three PQ masses, which we call $M_{N_s} \equiv M(sss)$ again with the same fixed \overline{m} . (This is analogous to the pseudoscalar η_s considered later.) These values are also given in Appendix B in Table 5. Using the fit function of eq. (20) and ignoring the \tilde{C}_1 and \tilde{C}_2 terms as discussed in section 3.1 gives the results in Table 1, together with the NNLO coefficient values

\tilde{A}_1	\tilde{A}_2	\tilde{B}_1	\tilde{B}_2	\tilde{B}_3
10.15(12)	1.828(157)	13.51(126)	-10.29(139)	-14.90(144)

Table 1: Results for the baryon octet expansion coefficients.

of $\tilde{C}_3 = -4.60(115)$, $\tilde{C}_4 = -17.5(26)$, $\tilde{C}_5 = -1.88(310)$ and $\tilde{C}_6 = -3.65(184)$. We note that in comparison to the NLO coefficients, the NNLO coefficients are poorly determined. The bootstrap (MINUIT) fit used gave $\chi^2/\text{dof} \sim 0.4$.

We now compare these results to a plot for illustration. The simplest to consider is setting $\delta\mu_a = \delta\mu_b$, i.e. degenerate valence quark masses. For simplicity, but slightly inaccurately, we shall in the following simply say $b = a$. (Of course we still need two different quark flavours.) With $\delta m_l = 0$, eq. (23) then becomes

$$\frac{\tilde{M}^2(aaa) - 1}{3\delta\mu_a} = \tilde{A}_1 + \tilde{B}_1\delta\mu_a + \frac{8}{3}\tilde{C}_3\delta\mu_a^2. \quad (28)$$

In Fig. 3 we plot $(\tilde{M}^2(aaa) - 1)/(3\delta\mu_a)$ against $\delta\mu_a$ for the PQ data (together with the cubic fit coefficients from Table 1) which due to the denominator is a sensitive plot. There is good agreement. (We postpone the comparison to the unitary data, ‘fan’ plots, until section 6.)

4 Octet pseudoscalar mesons

Determining the octet pseudoscalar mass splittings (or more accurately the splittings of the quadratic masses) will give δm_u^* , δm_d^* and δm_s^* (the quark masses at the physical point). This closely follows the baryon octet procedure, we must again consider the analogous flavour symmetry expansion for the pseudoscalar meson octet together with the known experimental masses of the pions and kaons.

In Fig. 4 we sketch the lowest pseudoscalar octet in the I_3 - Y plane. We have $K^0(d\bar{s})$, $K^+(u\bar{s})$, $\pi^+(u\bar{d})$ together with $\bar{K}^0(s\bar{d})$, $K^-(s\bar{u})$ and $\pi^-(d\bar{u})$ in the (outer) ring of the octet. From charge conjugation or C invariance we further have $M_{\bar{K}^0} = M_{K^0}$, $M_{K^-} = M_{K^+}$, and $M_{\pi^-} = M_{\pi^+}$ (which is in distinction to the baryon octet which does not have this constraint).

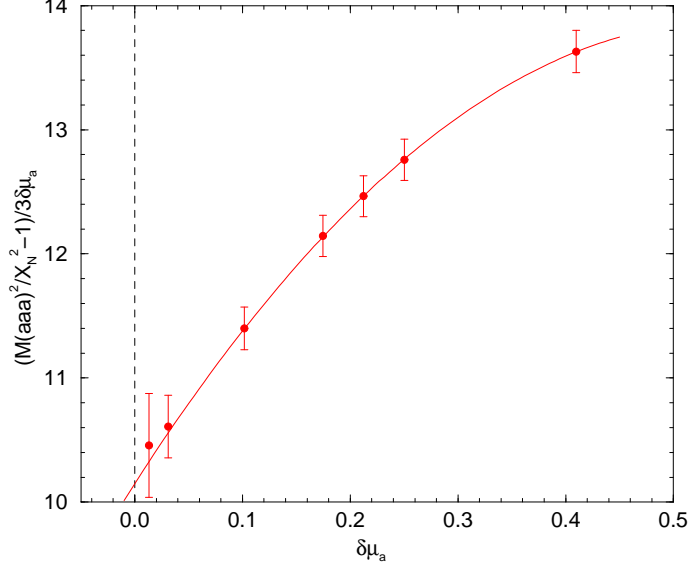


Figure 3: $(\tilde{M}^2(aaa) - 1)/(3\delta\mu_a)$ against $\delta\mu_a$, together with eq. (28) using the \tilde{A}_1, \tilde{B}_1 fit values from Table 1 and \tilde{C}_3 (given in the text).

4.1 PQ pseudoscalar meson flavour expansions

The corresponding formulas for the octet pseudoscalar mesons are simpler than for the octet baryon, due to the constraints imposed by C invariance. The following $SU(3)$ flavour breaking expansion formula is always valid for quarks $q = a, b, \dots$, in (u, d, s, \dots)

$$M^2(a\bar{b}) = M_{0\pi}^2 + \alpha(\delta m_a + \delta m_b) + \beta_0 \frac{1}{6}(\delta m_u^2 + \delta m_d^2 + \delta m_s^2) + \beta_1(\delta m_a^2 + \delta m_b^2) + \beta_2(\delta m_a - \delta m_b)^2, \quad (29)$$

in quark masses up to the NLO as discussed in [13]. (Note that $M(a\bar{b}) = M(b\bar{a})$.)

Again combinations of masses can be chosen, so that due to eq. (6) the linear term in eq. (29) vanishes, which is equivalent to averaging the outer ring of particles and finding the ‘centre of mass’ of the octet. In particular if we set

$$\begin{aligned} X_\pi^2 &= \frac{1}{6}(M_{K^+}^2 + M_{K^0}^2 + M_{\pi^+}^2 + M_{\pi^-}^2 + M_{K^0}^2 + M_{K^-}^2) \\ &= \frac{1}{3}(M_{K^+}^2 + M_{K^0}^2 + M_{\pi^+}^2), \end{aligned} \quad (30)$$

this gives

$$\begin{aligned} X_\pi^2 &= M_{0\pi}^2 + \left(\frac{1}{6}\beta_0 + \frac{2}{3}\beta_1 + \beta_2\right) (\delta m_u^2 + \delta m_d^2 + \delta m_s^2) \\ &= M_{0\pi}^2 + O(\delta m_q^2). \end{aligned} \quad (31)$$

In the partially quenched case, the above $SU(3)$ flavour expansion can be generalised to

$$M^2(a\bar{b}) = M_{0\pi}^2 + \alpha(\delta\mu_a + \delta\mu_b)$$

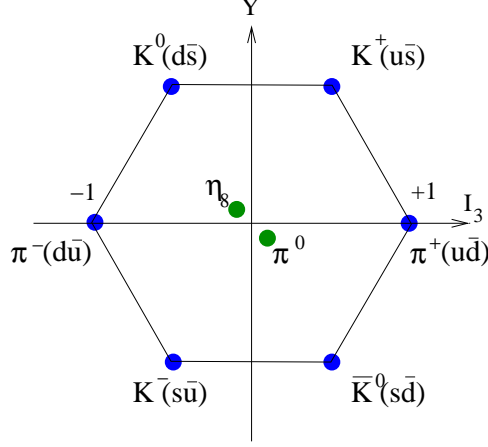


Figure 4: The lowest octet for the spin 0 pseudoscalar mesons plotted in the I_3 - Y plane.

$$\begin{aligned}
& + \beta_0 \frac{1}{6} (\delta m_u^2 + \delta m_d^2 + \delta m_s^2) + \beta_1 (\delta \mu_a^2 + \delta \mu_b^2) + \beta_2 (\delta \mu_a - \delta \mu_b)^2 \\
& + \gamma_0 \delta m_u \delta m_d \delta m_s + \gamma_1 (\delta \mu_a + \delta \mu_b) (\delta m_u^2 + \delta m_d^2 + \delta m_s^2) \\
& + \gamma_2 (\delta \mu_a + \delta \mu_b)^3 + \gamma_3 (\delta \mu_a + \delta \mu_b) (\delta \mu_a - \delta \mu_b)^2, \quad (32)
\end{aligned}$$

where the NLO was also discussed in [13] and again we have extended the formula to the NNLO case [14]. This is again a general formula valid for possibly differing masses of the sea, m_q , and valence quarks, μ_q . The same notation has been used as in sections 2 and 3. (In particular remember that $\delta \mu_q$ is unconstrained in distinction to the sea quarks, eq. (6). The unitary line is recovered when $\mu_q \rightarrow m_q$.) Again as with the PQ octet baryon case, eq. (18), we see that at the NNLO there is a term, the γ_1 term, which mixes the sea and valence quarks; as discussed in section 3.1 this again makes the numerical determination of these coefficients difficult (we cannot vary the sea quark masses over a large enough range). So in the same spirit as section 3.1 we ignore this term and regard the NNLO terms as ‘control’ terms.

If we wish to consider ‘physical ratios’ then the masses can again be conveniently normalised using X_π^2 . Expanding to NNLO, we find

$$\begin{aligned}
\tilde{M}^2(a\bar{b}) &= 1 + \tilde{\alpha} (\delta \mu_a + \delta \mu_b) \\
& - \left(\frac{2}{3} \tilde{\beta}_1 + \tilde{\beta}_2\right) (\delta m_u^2 + \delta m_d^2 + \delta m_s^2) + \tilde{\beta}_1 (\delta \mu_a^2 + \delta \mu_b^2) + \tilde{\beta}_2 (\delta \mu_a - \delta \mu_b)^2 \\
& + 2(\tilde{\gamma}_2 - 3\tilde{\gamma}_3) \delta m_u \delta m_d \delta m_s + \tilde{\gamma}_1 (\delta \mu_a + \delta \mu_b) (\delta m_u^2 + \delta m_d^2 + \delta m_s^2) \\
& + \tilde{\gamma}_2 (\delta \mu_a + \delta \mu_b)^3 + \tilde{\gamma}_3 (\delta \mu_a + \delta \mu_b) (\delta \mu_a - \delta \mu_b)^2, \quad (33)
\end{aligned}$$

where again a $\tilde{\sim}$ on a hadron mass squared means that it has been divided by X_π^2 (which only depends on the sea quarks) while on an expansion coefficient it means that the coefficient has been divided by $M_{0\pi}^2$ for example $\tilde{\alpha} = \alpha/M_{0\pi}^2$.

Again for a 2 + 1 flavour simulation (the case that will be considered here) eq. (33) slightly simplifies to become

$$\begin{aligned}
\tilde{M}^2(a\bar{b}) &= 1 + \tilde{\alpha}(\delta\mu_a + \delta\mu_b) \\
&\quad - 2(2\tilde{\beta}_1 + 3\tilde{\beta}_2)\delta m_l^2 + \tilde{\beta}_1(\delta\mu_a^2 + \delta\mu_b^2) + \tilde{\beta}_2(\delta\mu_a - \delta\mu_b)^2 \\
&\quad - 4(\tilde{\gamma}_2 - 3\tilde{\gamma}_3)\delta m_l^3 + 6\tilde{\gamma}_1(\delta\mu_a + \delta\mu_b)\delta m_l^2 \\
&\quad + \tilde{\gamma}_2(\delta\mu_a + \delta\mu_b)^3 + \tilde{\gamma}_3(\delta\mu_a + \delta\mu_b)(\delta\mu_a - \delta\mu_b)^2, \tag{34}
\end{aligned}$$

with the same coefficients, provided of course that \bar{m} remains constant and where

$$X_\pi^2 = \frac{1}{3}(2M^2(l\bar{5}) + M^2(l\bar{l})). \tag{35}$$

4.2 Determination of the coefficients

As in section 3 we need to consider PQ masses at the $SU(3)$ flavour symmetric point for the sea quark masses (see Table 6) jointly with the $32^3 \times 64$ lattice size unitary results from Table 20 of [13] all with the same \bar{m} constant value. From eq. (34) we need to determine the constants $\tilde{\alpha}$, $\tilde{\beta}_1$, $\tilde{\beta}_2$ and $\tilde{\gamma}_2$, $\tilde{\gamma}_3$.

A 5-parameter fit to the PQ and unitary data then yields the results of Table 2 together with the NNLO coefficient values of $\tilde{\gamma}_2 = -16.4(12)$ and $\tilde{\gamma}_3 = -20.3(39)$.

$\tilde{\alpha}$	$\tilde{\beta}_1$	$\tilde{\beta}_2$
41.17(8)	76.50(148)	-45.81(189)

Table 2: Results for the pseudoscalar octet expansion coefficients.

The bootstrap (MINUIT) fit used gave $\chi^2/\text{dof} \sim 1.7$.

As in section 3.2, it is useful to compare these fit results in a plot. In parallel to eq. (28) let us again consider the simple case of degenerate quark mass, i.e. where quark and antiquark have the same mass, but different flavours, so they cannot annihilate. We set $b = a$ and $\delta m_l = 0$ in eq. (34) and so consider

$$\frac{\tilde{M}^2(a\bar{a}) - 1}{2\delta\mu_a} = \tilde{\alpha} + \tilde{\beta}_1\delta\mu_a + 4\tilde{\gamma}_2\delta\mu_a^2. \tag{36}$$

In Fig. 5 we plot $(\tilde{M}^2(a\bar{a}) - 1)/(2\delta\mu_a)$ against $\delta\mu_a$ using the PQ data. This is compared with the cubic fit from eq. (36) and Table 2. There is good agreement.

4.3 Pseudoscalar meson isospin splittings

Having determined $\tilde{\alpha}$, $\tilde{\beta}_1$, $\tilde{\beta}_2$ we can now find δm_u , δm_d , δm_s given the masses around the outer ring of the pseudoscalar octet. We postpone a discussion of the numerical values until the next section and here just derive the relevant

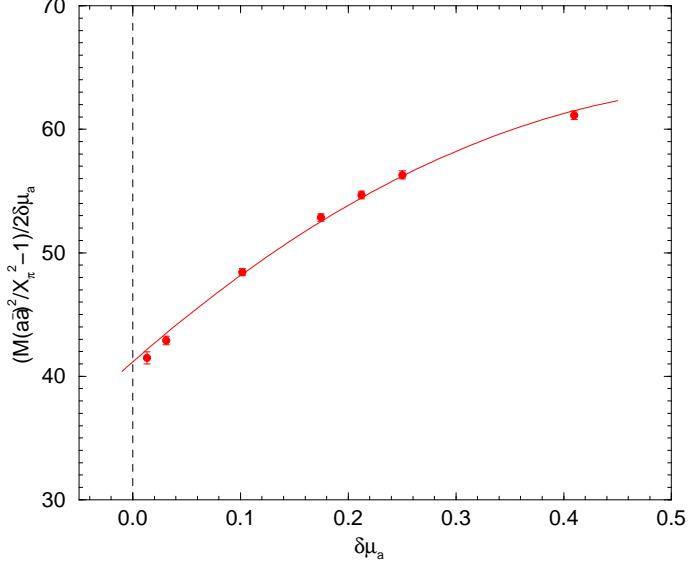


Figure 5: $(\tilde{M}^2(a\bar{a}) - 1)/(2\delta\mu_a)$ against $\delta\mu_a$. The full line is eq. (36), using the $\tilde{\alpha}$, $\tilde{\beta}_1$ fit values from Table 2 and $\tilde{\gamma}_2$ (given in the text).

formulas. As they are trivially valid over a range of quark masses (and not just at the physical point) we give these more general expressions here.

From eqs. (13)–(15) we see that we need $\delta m_d - \delta m_u \equiv \delta m_-$ and $\delta m_d + \delta m_u \equiv \delta m_+$. So as in section 2 we consider the mass difference

$$\begin{aligned} \tilde{M}_{K^0}^2 - \tilde{M}_{K^+}^2 &= (\delta m_d - \delta m_u)[\tilde{\alpha} + (\tilde{\beta}_1 + 3\tilde{\beta}_2)(\delta m_d + \delta m_u)] \\ &= \delta m_-[\tilde{\alpha} + (\tilde{\beta}_1 + 3\tilde{\beta}_2)\delta m_+]. \end{aligned} \quad (37)$$

Alternatively we can consider

$$\begin{aligned} \tilde{M}_{K^+}^2 - \tilde{M}_{\pi^+}^2 &= (\delta m_s - \delta m_d)[\tilde{\alpha} + (\tilde{\beta}_1 + 3\tilde{\beta}_2)(\delta m_s + \delta m_d)] \\ &= -\frac{1}{2}(\delta m_- + 3\delta m_+)[\tilde{\alpha} + \frac{1}{2}(\tilde{\beta}_1 + 3\tilde{\beta}_2)(\delta m_- - \delta m_+)], \end{aligned} \quad (38)$$

and

$$\begin{aligned} \tilde{M}_{K^0}^2 - \tilde{M}_{\pi^+}^2 &= (\delta m_s - \delta m_u)[\tilde{\alpha} + (\tilde{\beta}_1 + 3\tilde{\beta}_2)(\delta m_s + \delta m_u)] \\ &= \frac{1}{2}(\delta m_- - 3\delta m_+)[\tilde{\alpha} - \frac{1}{2}(\tilde{\beta}_1 + 3\tilde{\beta}_2)(\delta m_- + \delta m_+)], \end{aligned} \quad (39)$$

where we have used the constraint, eq. (6), to eliminate δm_s in the second line of eqs. (38) and (39) to re-write the equations in terms of δm_- , δm_+ .

Of course only two of the equations (37)–(39) are independent. Choosing eqs. (37) and (38), these quadratic equations can be solved iteratively to give δm_{\mp} . We start the iteration from the linear term alone or LO in the quark mass.

From eq. (37) we see that is sufficient to determine δm_+ to LO (and δm_- to NLO). Thus we find

$$\begin{aligned}\delta m_d - \delta m_u &= \frac{\tilde{M}_{K^0}^2 - \tilde{M}_{K^+}^2}{\tilde{\alpha}} \left(1 + \frac{2(\tilde{\beta}_1 + 3\tilde{\beta}_2)}{3\tilde{\alpha}^2} (\frac{1}{2}(\tilde{M}_{K^0}^2 + \tilde{M}_{K^+}^2) - \tilde{M}_{\pi^+}^2) \right), \\ \delta m_d + \delta m_u &= -\frac{2}{3\tilde{\alpha}} \left(\frac{1}{2}(\tilde{M}_{K^0}^2 + \tilde{M}_{K^+}^2) - \tilde{M}_{\pi^+}^2 \right) [1 + \epsilon_{NLO}].\end{aligned}\quad (40)$$

As $2(\tilde{\beta}_1 + 3\tilde{\beta}_2)/3\tilde{\alpha}^2 \sim -0.02$ then as, in particular, at the physical point $\frac{1}{2}(\tilde{M}_{K^0}^{*2} + \tilde{M}_{K^+}^{*2}) - \tilde{M}_{\pi^+}^{*2}$ is ~ 1 , we expect that the NLO term for δm_- is small,² i.e $\sim 3\%$ and tends to reduce the value of δm_- slightly. (See next section for the numerical values.)

5 Physical values of the quark masses

To proceed further we now need to substitute eqs. (40) into eqs. (13)–(15) to give the pure QCD contribution to baryon octet mass splittings in terms of the pseudoscalar octet masses.

Before considering this however (see section 7.1), we shall first discuss electromagnetic effects and determine the physical values of the quark masses δm_u^* and δm_d^* given the experimental values of the pseudoscalar masses. This will enable us to investigate the convergence of the $SU(3)$ flavour breaking expansion. The experimental masses are, [1],

$$\begin{aligned}M_{\pi^+}^{\text{exp}} &= 0.13957018(35) \text{ GeV}, \\ M_{K^0}^{\text{exp}} &= 0.497672(31) \text{ GeV}, \\ M_{K^+}^{\text{exp}} &= 0.493677(16) \text{ GeV},\end{aligned}\quad (41)$$

(with as already mentioned $M_{\bar{K}^0} = M_{K^0}$, $M_{K^-} = M_{K^+}$ and $M_{\pi^-} = M_{\pi^+}$), on the outer octet ring, and at the centre

$$M_{\pi^0}^{\text{exp}} = 0.1349766(6) \text{ GeV}.\quad (42)$$

We now need to consider electromagnetic effects (which may now be comparable to the $u - d$ quark mass difference which is also small). Electromagnetic effects tend to increase the mass of charged particles (due to the photon cloud).

²This is also true for δm_+ . The NLO term is

$$\epsilon_{NLO} = -\frac{\tilde{\beta}_1 + 3\tilde{\beta}_2}{3\tilde{\alpha}^2} \left(\frac{1}{2}(\tilde{M}_{K^0}^2 + \tilde{M}_{K^+}^2) - \tilde{M}_{\pi^+}^2 + 2(\tilde{M}_{K^0}^2 - \tilde{M}_{K^+}^2) - \frac{3(\tilde{M}_{K^0}^2 - \tilde{M}_{K^+}^2)^2}{\frac{1}{2}(\tilde{M}_{K^0}^2 + \tilde{M}_{K^+}^2) - \tilde{M}_{\pi^+}^2} \right).$$

Again together with $(\tilde{\beta}_1 + 3\tilde{\beta}_2)/3\tilde{\alpha}^2 \sim -0.01$ and $\frac{1}{2}(\tilde{M}_{K^0}^{*2} + \tilde{M}_{K^+}^{*2}) - \tilde{M}_{\pi^+}^{*2} \sim 1$, this means that the correction NLO term for δm_+ is also small.

As a help to estimate these unknown effects, we use Dashen’s theorem, [20], which states that if electromagnetic effects are the only source of breaking of isospin symmetry (i.e. $m_u = m_d$), the leading electromagnetic energy contribution to the neutral pseudoscalar particles, i.e. the π^0 , K^0 , vanishes, while that due to the charged particles, i.e. the π^+ , K^+ is equal. As the mass difference in π^0 and π^+ due to the $u - d$ quark mass difference is negligible, $O(0.1 \text{ MeV})$, e.g. [17], we can thus write (e.g. [21, 22])

$$\begin{aligned} M_{\pi^+}^{\text{exp } 2} &= M_{\pi^+}^{*2} + \mu_\gamma, & M_{\pi^0}^{\text{exp } 2} &= M_{\pi^0}^{*2} \equiv M_{\pi^+}^{*2}, \\ M_{K^+}^{\text{exp } 2} &= M_{K^+}^{*2} + \mu_\gamma, & M_{K^0}^{\text{exp } 2} &= M_{K^0}^{*2}. \end{aligned} \quad (43)$$

(The $*$ denotes values at the physical point for the pure QCD case.) Dashen’s theorem has corrections of $O(\alpha_{QED} m_q)$ from higher order terms. Sometimes possible violations of the theorem are parametrised by [4, 23]

$$M_{K^0}^{*2} - M_{K^+}^{*2} = (M_{K^0}^2 - M_{K^+}^2)^{\text{exp}} + (1 + \epsilon_\gamma) (M_{\pi^+}^2 - M_{\pi^0}^2)^{\text{exp}}, \quad (44)$$

where $\epsilon_\gamma = 0$ corresponds to Dashen’s theorem. For example a positive value for ϵ_γ would thus tend to increase slightly the value of $M_{K^0}^{*2} - M_{K^+}^{*2}$. From the first equation in eq. (40) this would only affect the leading term in our expansion, so our main result in section 7.2 will be given in terms of the kaon mass splitting, $M_{K^0}^{*2} - M_{K^+}^{*2}$ and where we shall consider ϵ_γ as an additional error.

Inverting the relations in eq. (43) gives [1]

$$M_{\pi^+}^{*2} = M_{\pi^0}^{\text{exp } 2}, \quad M_{K^+}^{*2} = M_{K^+}^{\text{exp } 2} - (M_{\pi^+}^{\text{exp } 2} - M_{\pi^0}^{\text{exp } 2}), \quad M_{K^0}^{*2} = M_{K^0}^{\text{exp } 2}, \quad (45)$$

or

$$M_{\pi^+}^* = 0.13498 \text{ GeV}, \quad M_{K^+}^* = 0.49240 \text{ GeV}, \quad M_{K^0}^* = 0.49767 \text{ GeV}, \quad (46)$$

which we shall use as the pure QCD values due to differences in the quark masses with the electromagnetic effects subtracted away (assuming Dashen’s theorem). This gives from eq. (30)³,

$$X_\pi^* = 0.4116 \text{ GeV}, \quad (47)$$

(of course this is very close to the experimental value of $X_\pi^{\text{exp}} = 0.4126 \text{ GeV}$).

In Table 3 using the masses given in eq. (46) we give our results, first giving the LO results for the quark masses, then the next line, NLO^a, gives the results from eq. (40), which we will be using here. As a check, the third line compares this NLO result to the NLO result using the Newton–Raphson method to iterate eqs. (37) and (38). We find the Newton–Raphson procedure converges very quickly (after

³In [13] we used the average kaon and pion masses as we were strictly in the 2 + 1 flavour case. Here we need to take into account the differences between charged and neutral mesons.

	$\delta m_d^* - \delta m_u^*$	$\delta m_d^* + \delta m_u^*$	δm_u^*	δm_d^*	δm_s^*
LO	0.0007485(14)	-0.02168(4)	-0.01121(2)	-0.01047(2)	0.02168(4)
NLO ^a	0.0007245(27)	-0.02204(6)	-0.01138(3)	-0.01066(3)	0.02204(6)
NLO ^b	<i>0.0007249</i>	<i>-0.02204</i>	<i>-0.01138</i>	<i>-0.01066</i>	<i>0.02204</i>

Table 3: Results for the bare quark mass in lattice units at the physical point using eq. (46) as input. The first line is the LO result. The next line, NLO^a, uses the result of eq. (40), while as a check the last line in italics, NLO^b, iterates eqs. (37) and (38).

one or two iterations) and find good agreement between the two results (well within the error bars of NLO^a in Table 3) and so we can be confident that eq. (40) is a good approximation for the inversion of eqs. (37) and (38).

We also note that the differences between the LO and NLO are small of the order of a few percent, indicating that the $SU(3)$ flavour expansion about the flavour symmetric point appears to be highly convergent. (We shall discuss this a little further in section 6.)

6 Comparison with ‘fan’ plots

We now compare the fit results with the mass values from previous ‘fan’ plots, [13], which describe the evolution of the pseudoscalar and baryon octet masses along a path from the $SU(3)$ symmetric point down to the physical point. In [13] the isospin degenerate limit, i.e. $m_u = m_d \equiv m_l$, was considered. So for this comparison we take the physical quark mass, in lattice units, as

$$\delta m_l^* \equiv \frac{1}{2}(\delta m_u^* + \delta m_d^*) = -0.01102(3). \quad (48)$$

In Fig. 6 we show numerical results between the $SU(3)$ flavour symmetric point and the ‘physical point’ for the numerical pseudoscalar octet on the unitary line (keeping $\overline{m} = \text{const.}$) from [13]. These masses are compared to the quadratic fit using eq. (34) (i.e. together with just the results of Table 2) for the 2+1 flavour case, i.e. $m_u = m_d = m_l$. The NNLO terms in the $SU(3)$ flavour symmetric expansion can be safely ignored in the small δm_l range. Compare the scale of the x -axis of Fig. 3 with that of Fig. 6. We consider $M_\pi(\overline{l\overline{l}})$, $M_K(l\overline{s})$ and the fictitious PQ particle η_s , with mass $M(s\overline{s})$. The comparison is satisfactory. We also show results from [13] on smaller $24^3 \times 48$ sized lattices. This shows that finite size effects for these ratios are rather small. Of course, the value of δm_l^* just serves to define pseudoscalar meson mass ratios at the ‘physical point’ in a $N_f = 2 + 1$ flavour world. For completeness we give these numbers here: $\tilde{M}_\pi^{*2} = 0.1077(26)$, $\tilde{M}_K^{*2} = 1.446(1)$ and $\tilde{M}_{\eta_s}^{*2} = 2.884(4)$.

In Fig. 7 we show the comparable baryon octet results. As well as considering the nucleon mass, $M_N(l\overline{l})$, we also show $M_\Sigma(l\overline{l}s)$, $M_\Xi(l\overline{l}s)$ and also a fictitious PQ

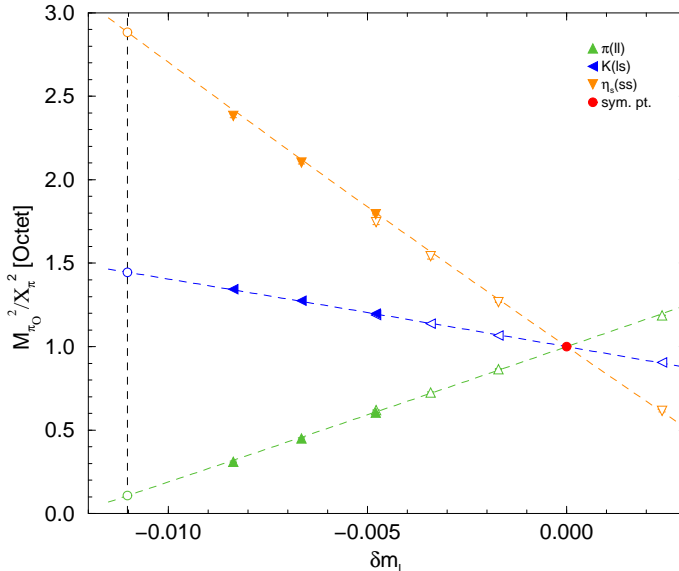


Figure 6: The pseudoscalar meson octet ‘fan’ plot, $M_{\pi_0}^2 / X_\pi^2$ ($\pi_O = \pi, K, \eta_s$) versus δm_l . The numerical mass values are taken from [13] where filled up triangles, left triangles, down triangles are $\pi(l)$, $K(ls)$, $\eta_s(ss)$ results respectively using $32^3 \times 64$ sized lattices. The common symmetric point is the filled circle. The opaque up triangles, left triangles, down triangles are from $24^3 \times 48$ sized lattices (and not used in the fits here). The quadratic fits are taken from eq. (34), together with Table 2. The vertical line from eq. (48) is the pure $N_f = 2 + 1$ QCD physical point, while the opaque circles are the pure QCD hadron mass ratios for $2 + 1$ quark flavours.

particle – $M_{N_s}(sss)$. Again the comparison of the NLO (quadratic) fit, using the expansion coefficient values given in Table 1, to the numerical data is satisfactory. For completeness we give here the values at the $2 + 1$ QCD physical point (opaque circles) of $\tilde{M}_N^{*2} = 0.6704(46)$, $\tilde{M}_\Sigma^{*2} = 1.051(6)$, $\tilde{M}_\Xi^{*2} = 1.278(8)$ and $\tilde{M}_{N_s}^{*2} = 1.692(9)$. For a comparison to these values, the stars in Fig. 7 represent the average of the squared masses of the appropriate particle, as defined in the figure caption.

7 Results and discussion

We are now in a position to numerically determine the baryon octet mass splittings due to pure QCD $u - d$ quark mass differences (see section 7.1, our main result), and then in section 7.2 estimate physical values for the splittings.

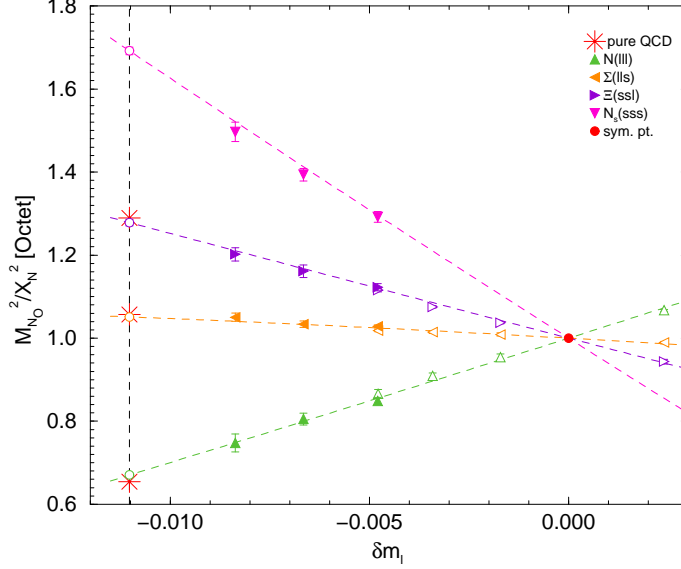


Figure 7: The baryon octet ‘fan’ plot, $M_{N_O}^2/X_N^2$ ($N_O = N, \Sigma, \Xi, N_s$) versus δm_l . The numerical mass values are taken from [13] where filled up-triangles, left-triangles, right-triangles, down-triangles are $N(III)$, $\Sigma(IIIs)$, $\Xi(ssl)$, $N_s(sss)$ results respectively using $32^3 \times 64$ sized lattices. The common symmetric point is the filled circle. The opaque up-triangles, left-triangles, right-triangles, down-triangles are from $24^3 \times 48$ sized lattices (and not used in the fits here). The quadratic fits are from eq. (23), together with Table 1. The vertical line from eq. (48) is the $N_f = 2 + 1$ pure QCD physical point, with the opaque circles being the determined pure QCD hadron mass ratios for $2 + 1$ quark flavours. For comparison, the stars represent the average of the squared masses of the appropriate particle on the outer ring of the baryon octet, Fig. 1, i.e. $M_N^{*2}(III) = (M_n^{\text{exp } 2}(ddu) + M_p^{\text{exp } 2}(uud))/2$, $M_\Sigma^{*2}(IIIs) = (M_{\Sigma^-}^{\text{exp } 2}(dds) + M_{\Sigma^+}^{\text{exp } 2}(uus))/2$, $M_\Xi^{*2}(ssl) = (M_{\Xi^-}^{\text{exp } 2}(ssd) + M_{\Xi^0}^{\text{exp } 2}(ssu))/2$.

7.1 Baryon octet mass splittings

After re-writing quark masses in terms of the pseudoscalar octet masses, section 4.3, and finding that the expansion is highly convergent in the relevant quark mass range, e.g. Table 3, we now insert the expansion of eq. (40) into eqs. (13)–(15) which gives the reasonably compact results

$$\tilde{M}_N - \tilde{M}_{N'} = \tilde{A}_{N-N'} \left[1 + \tilde{B}_{N-N'} \left(\frac{1}{2}(\tilde{M}_{K^0}^2 + \tilde{M}_{K^+}^2) - \tilde{M}_{\pi^+}^2 \right) \right] \left(\tilde{M}_{K^0}^2 - \tilde{M}_{K^+}^2 \right), \quad (49)$$

for the pairs $(N, N') = (n, p)$, (Σ^-, Σ^+) and (Ξ^-, Ξ^0) , where

$$\tilde{A}_{n-p} = \frac{\tilde{A}'_1 - 2\tilde{A}'_2}{\tilde{\alpha}}, \quad \tilde{B}_{n-p} = \frac{2}{3\tilde{\alpha}} \left(\frac{\tilde{\beta}_1 + 3\tilde{\beta}_2}{\tilde{\alpha}} - \frac{\tilde{B}'_1 - 2\tilde{B}'_2}{\tilde{A}'_1 - 2\tilde{A}'_2} \right), \quad (50)$$

together with

$$\tilde{A}_{\Sigma^- - \Sigma^+} = \frac{2\tilde{A}'_1 - \tilde{A}'_2}{\tilde{\alpha}}, \quad \tilde{B}_{\Sigma^- - \Sigma^+} = \frac{2}{3\tilde{\alpha}} \left(\frac{\tilde{\beta}_1 + 3\tilde{\beta}_2}{\tilde{\alpha}} - \frac{2\tilde{B}'_1 - \tilde{B}'_2 + 3\tilde{B}'_3}{2\tilde{A}'_1 - \tilde{A}'_2} \right), \quad (51)$$

and

$$\tilde{A}_{\Xi^- - \Xi^0} = \frac{\tilde{A}'_1 + \tilde{A}'_2}{\tilde{\alpha}}, \quad \tilde{B}_{\Xi^- - \Xi^0} = \frac{2}{3\tilde{\alpha}} \left(\frac{\tilde{\beta}_1 + 3\tilde{\beta}_2}{\tilde{\alpha}} - \frac{\tilde{B}'_1 + \tilde{B}'_2 + 3\tilde{B}'_3}{\tilde{A}'_1 + \tilde{A}'_2} \right). \quad (52)$$

As discussed before, as we have unknown electromagnetic effects, then we shall first present our results in a general form with (known) coefficients between the baryon and pseudoscalar meson splittings, within a pure QCD context. We now insert the numerically determined values from Tables 1 and 2 into eq. (49), together with eqs. (50)–(52), to give

$$\begin{aligned} \tilde{M}_n - \tilde{M}_p &= 0.0789(41)(8)(8)(32) \left(\tilde{M}_{K^0}^2 - \tilde{M}_{K^+}^2 \right) \\ &\times \left[1 + 0.0817(92) \left(\frac{1}{2}(\tilde{M}_{K^0}^2 + \tilde{M}_{K^+}^2) - \tilde{M}_{\pi^+}^2 \right) \right], \quad (53) \end{aligned}$$

together with

$$\begin{aligned} \tilde{M}_{\Sigma^-} - \tilde{M}_{\Sigma^+} &= 0.2243(35)(22)(2)(90) \left(\tilde{M}_{K^0}^2 - \tilde{M}_{K^+}^2 \right) \\ &\times \left[1 + 0.0077(30) \left(\frac{1}{2}(\tilde{M}_{K^0}^2 + \tilde{M}_{K^+}^2) - \tilde{M}_{\pi^+}^2 \right) \right], \quad (54) \end{aligned}$$

and

$$\begin{aligned} \tilde{M}_{\Xi^-} - \tilde{M}_{\Xi^0} &= 0.1455(24)(13)(6)(58) \left(\tilde{M}_{K^0}^2 - \tilde{M}_{K^+}^2 \right) \\ &\times \left[1 - 0.0324(50) \left(\frac{1}{2}(\tilde{M}_{K^0}^2 + \tilde{M}_{K^+}^2) - \tilde{M}_{\pi^+}^2 \right) \right], \quad (55) \end{aligned}$$

as our main numerical result. This is a pure QCD result: the isospin breaking is just due to the different masses of the u , d and s quarks. (To recapitulate, * means at the physical point and for the baryon octet $\tilde{M}_n = M_n/X_N$, etc. and for the pseudoscalar octet $\tilde{M}_{K^0} = M_{K^0}/X_\pi$, etc. where X^2 is the ‘average’ hadron (mass)² of the ‘outer’ ring of the octet, given numerically in eqs. (8) and (47).) Even with the long lever arm of PQ some of the NLO terms, i.e. for $\Sigma^- - \Sigma^+$ are only marginally determined.

The first error is statistical; the other errors are systematic as discussed in Appendix A. The second error bar is due to possible finite size effects, the third error estimates a possible error due to convergence of the $SU(3)$ flavour breaking expansion, while the last error is due to the choice of path to the physical point.

The above results are valid for a range of quark masses; we shall now specialise to the physical point, as discussed in section 5.

7.2 Physical values of the mass splittings

We first note that the NLO term is always small of the order of a few percent, and only slowly decreases for increasing number of strange quarks in the baryon. Using for the NLO term the mass values given in eq. (46) for the pure QCD case we have $\frac{1}{2}(\tilde{M}_{K^0}^{*2} + \tilde{M}_{K^+}^{*2}) - \tilde{M}_{\pi^+}^{*2} = 1.339$ (using the experimental rather than pure QCD masses would introduce negligible additional errors into the NLO term). In addition, using X_N^{*2} and X_π^{*2} from eqs. (8) and (47), this gives

$$\begin{aligned} M_n^* - M_p^* &= 0.599(32)(34) (M_{K^0}^{*2} - M_{K^+}^{*2}), \\ M_{\Sigma^-}^* - M_{\Sigma^+}^* &= 1.553(25)(63) (M_{K^0}^{*2} - M_{K^+}^{*2}), \\ M_{\Xi^-}^* - M_{\Xi^0}^* &= 0.954(18)(41) (M_{K^0}^{*2} - M_{K^+}^{*2}), \end{aligned} \quad (56)$$

where all masses in these equations are now in GeV, as our final result in terms of the pseudoscalar kaon masses. The first error is statistical, while the second is the total systematic error.

Using again the kaon values from eq. (46) and regarding possible violations of Dashen's theorem, eq. (44), as a further systematic error, our isospin breaking effects due to pure QCD alone (in MeV) are

$$\begin{aligned} M_n^* - M_p^* &= 3.13(15)(16)(76|\epsilon_\gamma|) \text{ MeV}, \\ M_{\Sigma^-}^* - M_{\Sigma^+}^* &= 8.10(14)(33)(193|\epsilon_\gamma|) \text{ MeV}, \\ M_{\Xi^-}^* - M_{\Xi^0}^* &= 4.98(10)(21)(120|\epsilon_\gamma|) \text{ MeV}. \end{aligned} \quad (57)$$

In general, comparing eq. (57) with eq. (3) would indicate that electromagnetic effects for $n - p$ are negative, for $\Sigma^- - \Sigma^+$ are small and for $\Xi^- - \Xi^0$ are positive.

The uncertainty due to ϵ_γ is the dominant error once we convert to MeV (i.e. unknown EM effects are the largest source of error). As an example, taking $\epsilon_\gamma = 0.7$, [4, 23] gives $M_n^* - M_p^* = 3.13(15)(16)(53) \text{ MeV}$, $M_{\Sigma^-}^* - M_{\Sigma^+}^* = 8.10(14)(33)(135) \text{ MeV}$ and $M_{\Xi^-}^* - M_{\Xi^0}^* = 4.98(10)(21)(84) \text{ MeV}$.

In [11], a determination of the $n - p$ isospin breaking effects due to electromagnetic effects was given, with a result of $-1.30(47) \text{ MeV}$. Adding this to the result of eq. (57) gives

$$(M_n - M_p)^{*+QED} = 1.83(52)(76|\epsilon_\gamma|) \text{ MeV}. \quad (58)$$

This is to be compared with the experimental result given in eq. (3) of 1.29 MeV . Thus we find consistency (within errors even with $|\epsilon_\gamma| \approx 0$). Thus this result also indicates that violations of Dashen's theorem seem to be small.

In Fig. 8 we compare this $n - p$ mass difference including QED, $(M_n - M_p)^{*+QED}$, eq. (58) with $\epsilon_\gamma = 0.7$, together the results of [2, 3, 4]. The filled circles use the QED determination of [11], while the filled square includes the full determination from that reference. Despite the fact that QED effects are treated slightly differently in each work, good agreement amongst the various determinations and with the experimental result is found.

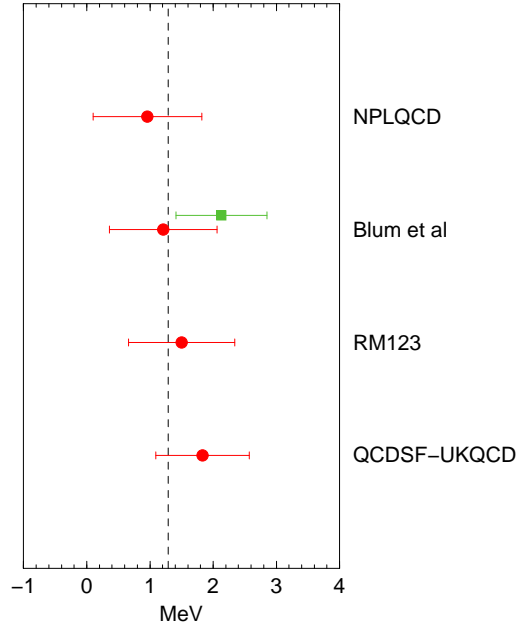


Figure 8: Comparison of the $n - p$ mass difference of the present result (QCDSF-UKQCD or lowest plotted number) with NPLQCD, Blum et al., and RM123 [2, 3, 4], respectively (top to bottom plotted numbers). The filled circles use the QED determination of [11], while the filled square gives the full QCD and QED determination from Blum et al. . The vertical dashed line is the experimental result given in eq. (3).

7.3 Conclusions

In this article we have introduced a method to determine the isospin breaking effects due to QCD for octet baryons. Using an $SU(3)$ flavour symmetry breaking expansion in the quark masses, the pseudoscalar meson octet expansion coefficients can be determined, which leads to an estimate at the physical quark mass point. This can then be used together with the equivalent $SU(3)$ flavour symmetry breaking expansion for the baryon octet to determine the baryon mass splittings. The expansion coefficients depend only on the average quark mass \bar{m} . Thus we can use degenerate sea quark masses (either with mass degenerate u and d quarks or with mass degenerate u , d and s quarks, i.e. at the flavour symmetric point) provided that \bar{m} remains unchanged. These are computationally cheaper simulations than those with mass non-degenerate u , d and s quarks.

A further advantage of our procedure is that the mass expansion formulas are easily generalised to the case of differing valence quark masses to sea quark masses (i.e. partially quenched valence quarks). This allows an extension of the quark mass range to heavier quark masses, so that both LO and NLO coefficients (i.e. linear terms and quadratic terms in quark masses) can be determined. Our final results are given in eq. (57). As the NLO turns out to be only a small

correction to the LO this gives us confidence that the $SU(3)$ flavour symmetry expansion appears to be a highly convergent series.

Acknowledgements

The numerical configuration generation was performed using the BQCD lattice QCD program [25] on the IBM BlueGeneL at EPCC (Edinburgh, UK), the BlueGeneL and P at NIC (Jülich, Germany), the SGI ICE 8200 at HLRN (Berlin-Hannover, Germany), and the JSCC (Moscow, Russia). The BlueGene codes were optimised using Bagel [26]. The Chroma software library [27] was used in the data analysis. This investigation has been supported partly by the DFG under Contract No. SFB/TR 55 (Hadron Physics from Lattice QCD) and by the EU Grants No. 227431 (Hadron Physics2), and No. 238353 (ITN STRONGnet). JN was partially supported by EU Grant No. 228398 (HPC-EUROPA2). JMZ is supported by the Australian Research Council Grant No. FT100100005. We thank all funding agencies.

Appendix

A Systematic errors

We now consider in this Appendix possible sources of systematic errors: finite lattice volume, convergence of the $SU(3)$ flavour breaking expansion, the path to the physical point and finite lattice spacing.

Finite lattice volume

Comparing the available $24^3 \times 48$ with the $32^3 \times 64$ lattice data in Fig. 7 indicates that for these mass ratios finite size effects are small. (Finite volume effects were also discussed in [13] in section 8.3.1.) We now use these unitary results to estimate possible finite size effects. For the lightest $24^3 \times 48$ point, namely, $(\kappa_l, \kappa_s) = (0.121040, 0.120620)$, $M_\pi L \sim 3.4$ (where L is the spatial lattice size, here $24a$), and the mass ratio \tilde{M} has finite size error $\sim 1\%$, from comparing the $24^3 \times 48$ lattice result with the $32^3 \times 64$ lattice result. (Either using the results of [13] directly or equivalently taking the square root of the results in Fig. 7.) On the lightest $32^3 \times 64$ lattice point, namely $(0.121145, 0.120413)$ we have $M_\pi L \sim 3.1$, so we expect the finite size errors in the mass ratio \tilde{M}_N will be approximately the same, i.e. also $\sim 1\%$. We use this in section 7 to estimate systematic errors arising from finite volume effects.

$SU(3)$ flavour breaking expansion

We first note that in Fig. 7 in the range $|\delta m_l| \lesssim 0.01$ (and $|\delta m_s| \lesssim 0.02$), there is little curvature. This is in agreement with the $SU(3)$ flavour breaking expansion, eq. (10), where each order is multiplied by a further δm_q . From Table 1 for the \tilde{A}_i and \tilde{B}_i coefficients (and for the NNLO order the \tilde{C}_i coefficients) we see there that they remain approximately all of the same order, so we expect that every increase in the order leads to a decrease by about an order of magnitude in the series. This is confirmed in the present case as we have compared the NNLO determination of M_N , M_Σ and M_Ξ with the NLO results (removing the heavier quark mass points until the χ^2/dof is approximately the same). The change in M_N was less than half a percent and for M_Σ , M_Ξ less, which is equivalent to using $\sim 10\%$ of the NLO term to estimate systematic errors.

A further example to illustrate this convergence is given by eq. (42) of [13]. Here we can form sums and differences of the decuplet masses which are of order δm_l^0 , δm_l^1 , δm_l^2 and δm_l^3 . We see that each time we add a factor of δm_l the quantity decreases by an order of magnitude (in fact usually by a factor of ~ 20), and the $O(\delta m_l^3)$ quantity is about 2000 times smaller than the leading order quantity. So we believe that convergence is very good for hyperons. Such an expansion is very good compared to most approaches available to QCD.

Path to physical point

As also discussed in [13], the chosen trajectory in the $m_s - m_l$ plane (keeping \bar{m} constant), appears to not quite go through the physical point. Using X_π (see eq. (35)) and X_N then from Table 15 of [13], we see that $(aX_\pi/aX_N) \times (X_N/X_\pi)^*$ deviates from 1 by $\sim 4\%$. We use this as an estimate in section 7 of systematic errors due to this effect.

Finite lattice spacing

Non-perturbative $O(a)$ improved clover fermions are employed in order to minimise finite lattice spacing effects in the mass ratios determined here. Any effects are difficult to estimate if only one β (or a value) is available, so as a check we have performed some additional simulations at $\beta = 5.80$ (with an estimated $a \sim 0.06$ fm). The results are along the $SU(3)$ flavour symmetric line (as three light quarks might show effects sooner than two light and one heavier quark). Again we have located (as described in [13]) the starting point on this line, m_0 for a path in the $m_s - m_l$ plane leading to the physical point and then considered comparable mass ratios for the nucleon, $X_N^2(\bar{m})/X_N^2(m_0)$ (against $X_\pi^2(\bar{m})/X_\pi^2(m_0)$), where we denote here a general point on the $SU(3)$ symmetric line by \bar{m} . In Fig. 9 we show these results. Both β values lie on a common line and show no

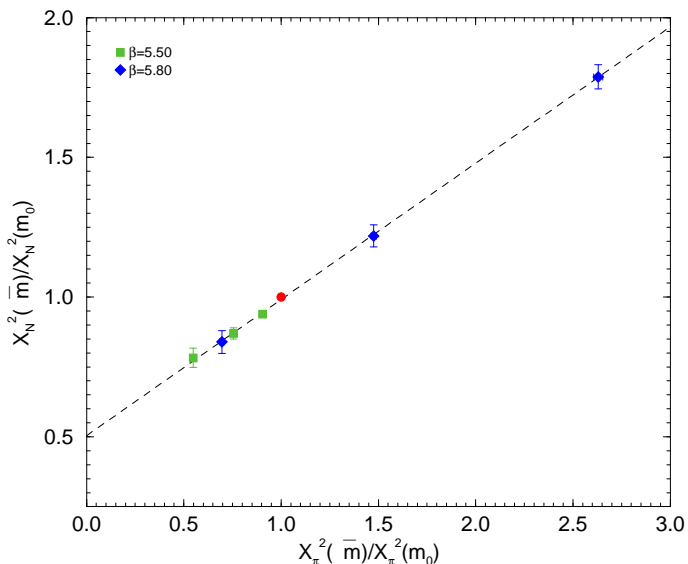


Figure 9: $X_N^2(\bar{m})/X_N^2(m_0)$ against $X_\pi^2(\bar{m})/X_\pi^2(m_0)$ along the symmetric line. Square symbols are the $\beta = 5.50$ results and are given in [13] and [24], while diamonds are the $\beta = 5.80$ results [14]. (All results are on $32^3 \times 64$ sized lattices.) The point where $m_0 = \bar{m}$ ($\kappa_0 = 0.12090$ for $\beta = 5.50$ and $\kappa_0 = 0.12281$ for $\beta = 5.80$) is denoted by a circle.

systematic lattice spacing dependence and so lie close to the continuum limit (certainly within the precision achievable here).

B Tables

We now give in Tables 4 – 6 the baryon and pseudoscalar PQ mass results used in the analysis. Additional $32^3 \times 64$ results along the line $\overline{m} = \text{const.}$ also used here are given in Tables 22 and 20 of [13] for the baryon and pseudoscalar meson particles, respectively.

κ_a	κ_b	$M(aab)$
0.110000	0.110000	1.969(3)
0.110000	0.115000	1.780(3)
0.110000	0.120000	1.555(3)
0.110000	0.120512	1.530(3)
0.110000	0.120900	1.511(3)
0.114000	0.114000	1.520(3)
0.114000	0.116000	1.436(3)
0.114000	0.118000	1.345(3)
0.114000	0.120000	1.245(3)
0.114000	0.120900	1.199(3)
0.115000	0.110000	1.592(3)
0.115000	0.115000	1.397(3)
0.115000	0.120000	1.161(2)
0.115000	0.120512	1.133(2)
0.115000	0.120900	1.113(3)
0.116000	0.114000	1.354(3)
0.116000	0.116000	1.268(3)
0.116000	0.118000	1.175(3)
0.116000	0.120000	1.072(3)
0.116000	0.120900	1.023(2)
0.118000	0.114000	1.173(3)
0.118000	0.116000	1.085(3)
0.118000	0.118000	0.9887(25)
0.118000	0.120000	0.8800(23)
0.118000	0.120900	0.8267(23)

Table 4: Results for the PQ baryon masses, $M(aab)$ in lattice units at $\beta = 5.50$ from a $32^3 \times 64$ lattice with sea quark masses at the symmetric point, i.e. $\kappa_l = \kappa_s = 0.12090$ and valence quarks κ_a, κ_b .

κ_a	κ_b	$M(aab)$
0.120000	0.110000	1.134(3)
0.120000	0.114000	0.9726(26)
0.120000	0.115000	0.9279(24)
0.120000	0.116000	0.8812(24)
0.120000	0.118000	0.7789(23)
0.120000	0.120000	0.6588(23)
0.120000	0.120512	0.6232(24)
0.120000	0.120900	0.5945(26)
0.120512	0.110000	1.081(3)
0.120512	0.115000	0.8722(25)
0.120512	0.120000	0.5945(25)
0.120512	0.120512	0.5564(27)
0.120512	0.120900	0.5247(30)
0.120900	0.110000	1.041(4)
0.120900	0.114000	0.8755(36)
0.120900	0.115000	0.8295(32)
0.120900	0.116000	0.7811(34)
0.120900	0.118000	0.6739(33)
0.120900	0.120000	0.5435(32)
0.120900	0.120512	0.5031(35)
0.120900	0.120900	0.4673(27)

Table 4 continued.

κ_l	κ_s	$M(sss)$
0.121040	0.120620	0.5265(16)
0.121095	0.120512	0.5446(16)
0.121145	0.120413	0.5682(13)

Table 5: Additional results to Table 22 of [13] for the PQ baryon masses, $M_{N_s} \equiv M(sss)$ in lattice units from a $32^3 \times 64$ lattice along the line $\overline{m} = \text{const.}$.

κ_a	κ_b	$M(a\bar{b})$
0.110000	0.110000	1.2485(3)
0.110000	0.115000	1.0583(3)
0.110000	0.120000	0.8351(4)
0.110000	0.120900	0.7909(10)
0.110000	0.120512	0.8100(6)
0.114000	0.114000	0.9436(3)
0.114000	0.116000	0.8583(3)
0.114000	0.118000	0.7664(3)
0.114000	0.120000	0.6669(4)
0.114000	0.120900	0.6200(7)
0.115000	0.115000	0.8593(3)
0.115000	0.120000	0.6202(4)
0.115000	0.120900	0.5720(6)
0.115000	0.120512	0.5929(5)
0.116000	0.116000	0.7706(3)
0.116000	0.118000	0.6754(3)
0.116000	0.120000	0.5710(4)
0.116000	0.120900	0.5213(6)
0.118000	0.118000	0.5752(3)
0.118000	0.120000	0.4628(4)
0.118000	0.120900	0.4077(5)
0.120000	0.120000	0.3342(4)
0.120000	0.120900	0.2646(5)
0.120000	0.120512	0.2958(4)
0.120512	0.120900	0.2174(5)
0.120512	0.120512	0.2534(4)
0.120900	0.120900	0.1747(5)

Table 6: Results for the PQ pseudoscalar masses, $M(a\bar{b})$ in lattice units at $\beta = 5.50$ from a $32^3 \times 64$ lattice with sea quark masses at the symmetric point, i.e. $\kappa_l = \kappa_s = 0.12090$ and valence quarks κ_a, κ_b .

References

- [1] K. Nakamura et al. (Particle Data Group), *J. Phys. G* **37** (2010) 075021.
- [2] S. R. Beane, K. Orginos, and M. J. Savage, *Nucl. Phys.* **B768** (2007) 38, [arXiv:hep-lat/0605014].
- [3] T. Blum, T. Doi, M. Hayakawa, T. Izubuchi, S. Uno, N. Yamada, and R. Zhou, *Phys. Rev. D* **82** (2010) 094508, [arXiv:1006.1311 [hep-lat]].
- [4] G. M. de Divitiis, P. Dimopoulos, R. Frezzotti, V. Lubicz, G. Martinelli, R. Petronzio, G. C. Rossi, F. Sanfilippo, S. Simula, N. Tantalo, and C. Tarantino, [RM123 Collaboration], *J. High Energy Phys.* **04** (2012) 124, [arXiv:1110.6294 [hep-lat]]; *PoS(Lattice 2011)* (2011) 291, arXiv:1202.5222 [hep-lat].
- [5] A. Duncan, E. Eichten, and H. Thacker, *Phys. Rev. Lett.* **76** (1996) 3894, [arXiv:hep-lat/9602005].
- [6] T. Blum, T. Doi, M. Hayakawa, T. Izubuchi, and N. Yamada, *Phys. Rev. D* **76** (2007) 114508, [arXiv:0708.0484 [hep-lat]].
- [7] S. Basak, A. Bazavov, C. Bernard, C. DeTar, W. Freeman, S. Gottlieb, U. M. Heller, J. E. Hetrick, J. Laiho, L. Levkova, J. Osborn, R. Sugar, and D. Toussaint, *PoS(LATTICE2008)* (2008) 127, arXiv:0812.4486 [hep-lat].
- [8] A. Portelli, S. Dürr, Z. Fodor, J. Frison, C. Hoelbling, S. D. Katz, S. Krieg, T. Kurth, L. Lellouch, T. Lippert, A. Ramos and K. K. Szabó, *PoS(Lattice 2011)* (2011) 136, arXiv:1201.2787 [hep-lat].
- [9] B. Glaessle and G. S. Bali, *PoS(Lattice 2011)* (2011) 282, arXiv:1111.3958 [hep-lat].
- [10] S. Aoki, K.-I. Ishikawa, N. Ishizuka, K. Kanaya, Y. Kuramashi, Y. Nakamura, Y. Namekawa, M. Okawa, Y. Taniguchi, A. Ukawa, N. Ukita and T. Yoshié, [PACS-CS Collaboration] *Phys. Rev.* **D86** (2012) 034507, [arXiv:1205.2961 [hep-lat]]; N. Ukita, *PoS(Lattice 2011)* (2011) 144, arXiv:1111.6380 [hep-lat].
- [11] A. Walker-Loud, C. E. Carlson and G. A. Miller, *Phys. Rev. Lett.* **108** (2012) 232301, [arXiv:1203.0254 [nucl-th]].
- [12] W. Bietenholz, V. Bornyakov, N. Cundy, M. Göckeler, R. Horsley, A. D. Kennedy, W. G. Lockhart, Y. Nakamura, H. Perlt, D. Pleiter, P. E. L. Rakow, A. Schäfer, G. Schierholz, A. Schiller, H. Stüben, and J. M. Zanotti, *Phys. Lett. B* **690** (2010) 436, [arXiv:1003.1114 [hep-lat]].

- [13] W. Bietenholz, V. Bornyakov, M. Göckeler, R. Horsley, W. G. Lockhart, Y. Nakamura, H. Perlt, D. Pleiter, P. E. L. Rakow, G. Schierholz, A. Schiller, T. Streuer, H. Stüben, F. Winter, and J. M. Zanotti, [QCDSF–UKQCD Collaboration], *Phys. Rev. D* **84** (2011) 054509, [[arXiv:1102.5300 \[hep-lat\]](#)].
- [14] QCDSF–UKQCD Collaboration, in preparation.
- [15] M. Gell-Mann, *Phys. Rev.* **125** (1962) 1067.
- [16] S. Okubo, *Prog. Theor. Phys.* **27** (1962) 949.
- [17] J. Gasser and H. Leutwyler, *Phys. Rep.* **87** (1982) 77.
- [18] S. Coleman and S. L. Glashow, *Phys. Rev. Lett.* **6** (1961) 423.
- [19] N. Cundy, M. Göckeler, R. Horsley, T. Kaltenbrunner, A. D. Kennedy, Y. Nakamura, H. Perlt, D. Pleiter, P. E. L. Rakow, A. Schäfer, G. Schierholz, A. Schiller, H. Stüben, and J. M. Zanotti, [QCDSF–UKQCD Collaboration], *Phys. Rev. D* **79** (2009) 094507, [[arXiv:0901.3302 \[hep-lat\]](#)].
- [20] R. Dashen, *Phys. Rev.* **183** (1969) 1245.
- [21] T-P. Cheng and L-F. Li, *Gauge Theory of Elementary Particle Physics*, Oxford University Press (1984).
- [22] H. Leutwyler, *Nucl. Phys. Proc. Suppl.* **94** (2001) 108, [arXiv:hep-ph/0011049](#).
- [23] G. Colangelo, S. Dürr, A. Jüttner, L. Lellouch, H. Leutwyler, V. Lubicz, S. Necco, C. T. Sachrajda, S. Simula, A. Vladikas, U. Wenger, and H. Wittig, [FLAG (Flavianet Lattice Averaging Group)], *Eur. Phys. J. C* **71** (2011) 1695, [[arXiv:1011.4408 \[hep-lat\]](#)].
- [24] R. Horsley, Y. Nakamura, H. Perlt, D. Pleiter, P.E.L. Rakow, G. Schierholz, A. Schiller, H. Stüben, F. Winter, J. M. Zanotti [QCDSF–UKQCD Collaboration], *Phys. Rev. D* **85** (2012) 034506, [[arXiv:1110.4971 \[hep-lat\]](#)].
- [25] Y. Nakamura and H. Stüben, *PoS(Lattice 2010)* (2010) 040, [arXiv:1011.0199 \[hep-lat\]](#).
- [26] P. A. Boyle, *Comp. Phys. Comm.* **180** (2009) 2739.
- [27] R. G. Edwards and B. Joó, *Nucl. Phys. Proc. Suppl.* **140** (2005) 832, [arXiv:hep-lat/0409003](#).